

THE TEMPERATURE DEPENDENCE OF THE ELECTRIC FIELD GRADIENT IN FERRICYANIDES

A. Z. HRYNKIEWICZ^{*,**}, B. D. SAWICKA^{*}, J. A. SAWICKI^{**}Institute of Nuclear Physics, Cracow^{*}Institute of Physics, Jagellonian University, Cracow^{**}*(Received December 12, 1969)*

The quadrupole splittings of the Mössbauer absorption spectra of ^{57}Fe in ferricyanides $\text{Me}_3[\text{Fe}(\text{CN})_6]_2$ (Me: Mn, Co, Ni, Cu, Cd and Ca) were studied from 4.2°K to over 400°K. Low temperature limiting values of the splitting $2\varepsilon(0^\circ\text{K})$ were found to be 0.92, 0.79, 0.96, 0.80, 0.95 and 0.49 mm/s respectively. The observed strong temperature dependence is interpreted in terms of the temperature dependent occupation probabilities of the hole in the t_{2g}^5 shell of the ferric ion. The distances between singlet and doublet orbital states were determined. The role of lattice contribution to the electric field gradient is taken into account. In $\text{Cr}[\text{Fe}(\text{CN})_6]$, $\text{Ti}[\text{Fe}(\text{CN})_6]$ and $\text{V}_3[\text{Fe}(\text{CN})_6]_4$ cubic structures the quadrupole splitting is negligible ($2\varepsilon < 0.20$ mm/s).

Introduction

The electronic structure of a ferric ion in the ferricyanide complex $[\text{Fe}^{\text{III}}(\text{CN})_6]$ is radically different from the structure of the Fe^{3+} ion in ionic compounds. Because of strong covalent bonding between the central iron ion and surrounding CN^- ligands Hund's principle is violated; the $3d^5$ -electrons of the ferric ion occupy the lower t_{2g} orbitals and the effective spin is low, viz., $S = 1/2$. This has been explained simply in terms of crystalline field theory (the case of a strong crystal field) and more accurately by means of molecular orbital theory (back donation and dative bonds).

The hyperfine interactions in low-spin iron ions are also considerably modified as compared with those of high-spin iron ions. For instance, if in high-spin Fe^{3+} complexes the electric field gradient acting on the iron nuclei is of lattice origin, then in low-spin ferricyanide complexes it is mainly produced by $3d^5$ -electrons of iron ion.

* Address: Instytut Fizyki Jądrowej, Kraków 23, Radzikowskiego 152, Polska.

** Address: Instytut Fizyki, Uniwersytet Jagielloński, Kraków 16, Reymonta 4, Polska.

The temperature dependence of quadrupole splitting in some ferricyanides of $\text{Me}_3[\text{Fe}(\text{CN})_6]_2$ type down to liquid helium temperature were measured previously with the Mössbauer effect method [1]. In this work we wish to report on a systematic experimental study of the quadrupole interactions in cubic ferricyanide complexes, their temperature variations their limiting values, and comparison with theory.

Experimental results

The samples of ferricyanides $\text{Me}_3^{2+}[\text{Fe}(\text{CN})_6]_2$ (Me denoting Mn, Co, Ni, Cu, Cd or Ca), $\text{Me}^{3+}[\text{Fe}(\text{CN})_6]$ (Me: Cr, Ti) and $\text{V}_3^{4+}[\text{Fe}(\text{CN})_6]_4$ were prepared from $\text{K}_3[\text{Fe}(\text{CN})_6]$ and the appropriate metal chlorides. As has been established [2], [3] and confirmed by our X-ray

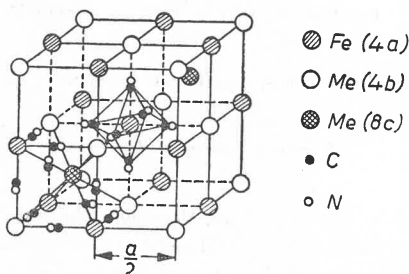


Fig. 1. Crystal structure of the cubic ferricyanides

tests, the investigated ferricyanides are of face-centred cubic structure, $O_h^5 - Fm\bar{3}m$. The crystal structure of the cubic ferricyanides is presented in Fig. 1.

Measurements of Mössbauer spectra were performed in the temperature range from 4.2°K to over 400°K. The quadrupole splittings 2ϵ were determined by least squares fitting of two Lorentzian lines to the observed spectra. In Figs 2 to 7 the quadrupole splitting data *vs.* temperature in measured ferricyanides are given.

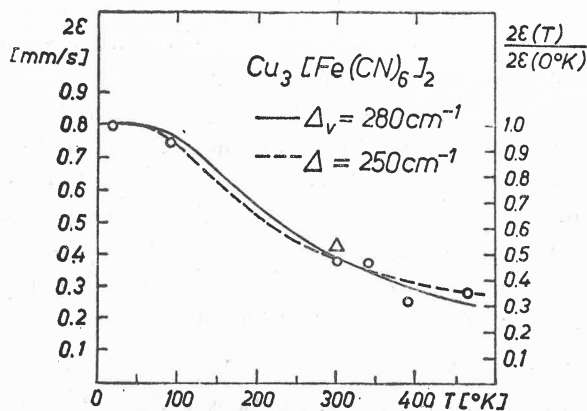


Fig. 2. Quadrupole splitting data against temperature in $\text{Cu}_3[\text{Fe}(\text{CN})_6]_2$

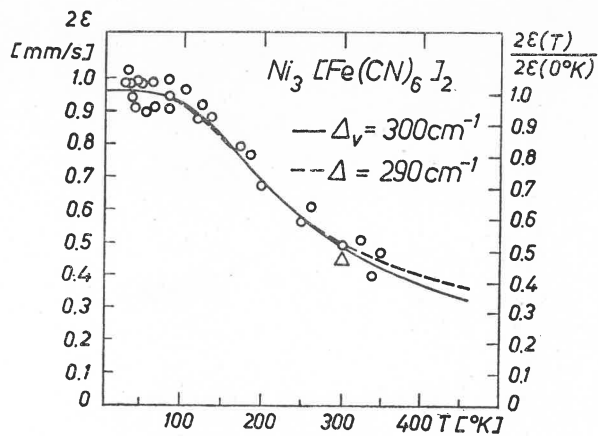


Fig. 3. Quadrupole splitting data against temperature in $\text{Ni}_3[\text{Fe}(\text{CN})_6]_2$

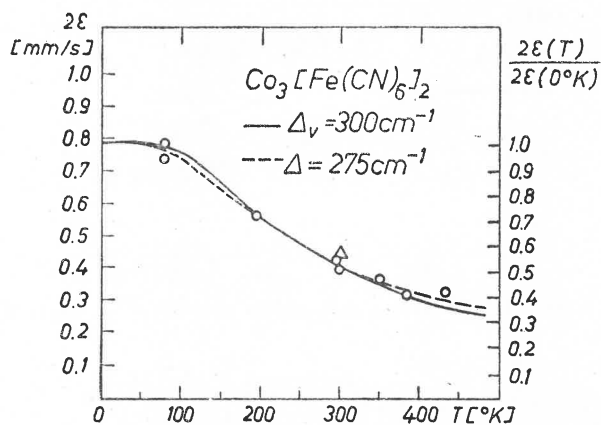


Fig. 4. Quadrupole splitting data against temperature in $\text{Co}_3[\text{Fe}(\text{CN})_6]_2$

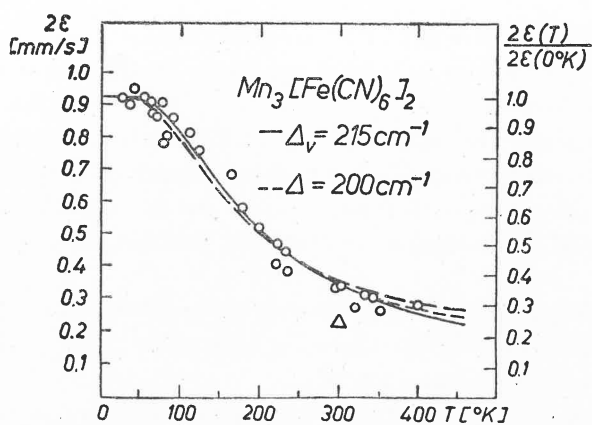


Fig. 5. Quadrupole splitting data against temperature in $\text{Mn}_3[\text{Fe}(\text{CN})_6]_2$

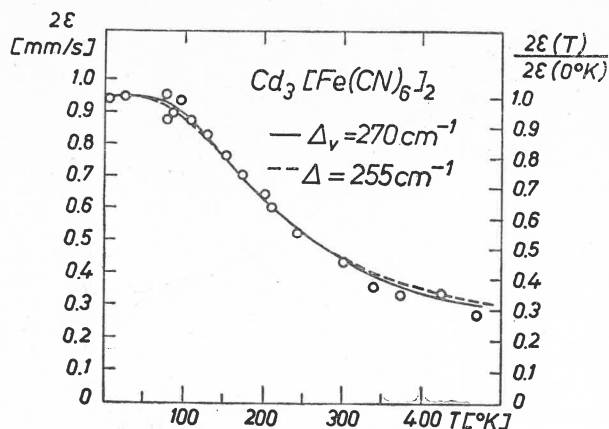


Fig. 6. Quadrupole splitting data against temperature in $\text{Cd}_3[\text{Fe}(\text{CN})_6]_2$

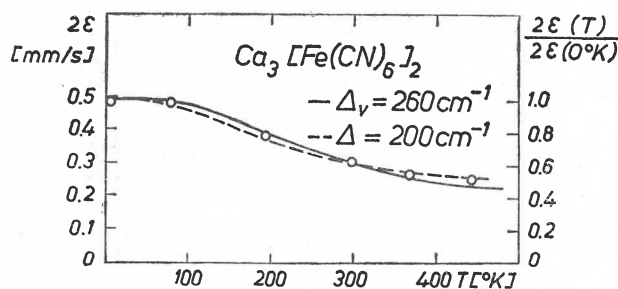


Fig. 7. Quadrupole splitting data against temperature in $\text{Ca}_3[\text{Fe}(\text{CN})_6]_2$

Discussion

The temperature dependences of quadrupole splittings in all investigated ferricyanides are compared in Fig. 8. The experimental results for $\text{K}_3[\text{Fe}(\text{CN})_6]$ Ref. [4] are also included.

The observed trends may be generally explained as follows. In the case of $\text{Me}_3[\text{Fe}(\text{CN})_6]_2$ structure the degeneracy of the t_{2g} level of the ferric ion is removed by a low-symmetry crystal field generated by Me^{2+} ions at the 8c: (1/4, 1/4, 1/4) and (3/4, 3/4, 3/4) positions and a spin-orbit coupling. The temperature dependent electron population on t_{2g} sublevels produces a relatively strong temperature dependent electric field gradient. In the case of $\text{Me}[\text{Fe}(\text{CN})_6]$ and $\text{V}_3[\text{Fe}(\text{CN})_6]_4$ structures, in which the 8c positions are not occupied and the cubic symmetry of iron positions is maintained, the Mössbauer spectra have the form of single lines.

In order to explain the temperature variation of the electric field gradient quantitatively Ingalls' theory [5], developed for the high-spin ferrous ion ($t_{2g}^4 e_g^2$), has been modified to describe the case of low-spin ferric ion (t_{2g}^5).

Considering the relation between holes and electrons, we have to take the t_{2g}^5 electron configuration as a t_{2g}^1 hole configuration. Let us denote the relative separations between the

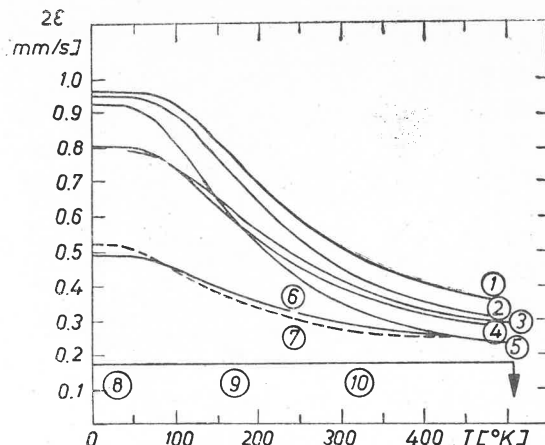


Fig. 8. Temperature dependences of quadrupole splittings in ferricyanides. 1) $\text{Ni}_3[\text{Fe}(\text{CN})_6]_2$, 2) $\text{Cd}_3[\text{Fe}(\text{CN})_6]_2$, 3) $\text{Co}_3[\text{Fe}(\text{CN})_6]_2$, 4) $\text{Cu}_3[\text{Fe}(\text{CN})_6]_2$, 5) $\text{Mn}_3[\text{Fe}(\text{CN})_6]_2$, 6) $\text{Ca}_3[\text{Fe}(\text{CN})_6]_2$, 7) $\text{K}_3[\text{Fe}(\text{CN})_6]$, 8) $\text{Cr}[\text{Fe}(\text{CN})_6]$, 9) $\text{Ti}[\text{Fe}(\text{CN})_6]$, 10) $\text{V}_3[\text{Fe}(\text{CN})_6]_4$

upper and lower sub-levels $|xy\rangle$, $|yz\rangle$, $|xz\rangle$ of the t_{2g} state by Δ_1 and Δ_2 . Taking into account the temperature dependent probabilities of a hole occupying the $|xy\rangle$, $|yz\rangle$ and $|xz\rangle$ levels, the temperature dependence of the valence electric field gradient q_v can be described by the F' factor:

$$F' = \frac{[1 + e^{-2\Delta_1/kT} + e^{-2\Delta_2/kT} - e^{-\Delta_1/kT} - e^{-\Delta_2/kT} - e^{-(\Delta_1+\Delta_2)/kT}]^{1/2}}{1 + e^{-\Delta_1/kT} + e^{-\Delta_2/kT}}$$

$$F' = 2\varepsilon_v(T)/2\varepsilon_v(0^\circ\text{K}).$$

Computations of the $F'(\Delta_1, \Delta_2, T)$ factor have been made. The results in the case of axially symmetrical crystal field are presented in Figs 9 and 10. It can be seen that F' factor is very sensitive to small variations of Δ and over the T range from 0°K to 400°K changes considerably.

The F' factor is equal to one at zero temperature if an upper state is orbitally non-degenerate ($\Delta_1 = \Delta_2 = \Delta$ in the axial case). It becomes equal to 1/2 if an upper state is degenerate ($\Delta_1 = 0$ or $\Delta_2 = 0$). These two cases are actually observed experimentally. The limiting $2\varepsilon(0^\circ\text{K})$ values of quadrupole splitting at low temperatures in $\text{Ca}_3[\text{Fe}(\text{CN})_6]_2$ and $\text{K}_3[\text{Fe}(\text{CN})_6]$ are almost twice smaller than in the other ferricyanides (see Fig. 8).

By fitting the $F'(\Delta, T)$ curve to the experimental $2\varepsilon(T)/2\varepsilon(0^\circ\text{K})$ results we determine the Δ -parameters to get the best agreement (the continuous lines in Figs 2 to 7). The axial case proved to be the best in all fitting procedures. As can be seen, the agreement of calculated curves with experimental results is quite satisfactory.

To estimate the role of the lattice electric field gradient for $\text{Me}_3[\text{Fe}(\text{CN})_6]_2$ lattices it has been computed in point charge approximation. The resulting \hat{q}_l tensor being axial with

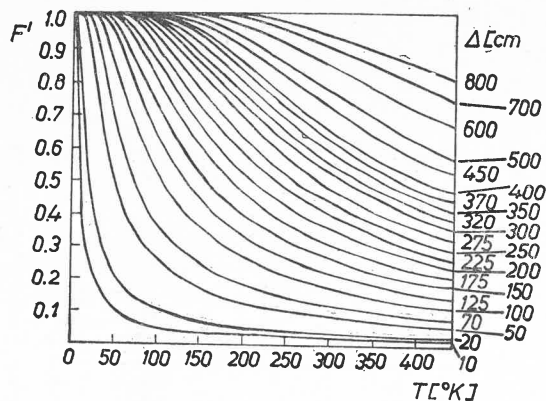


Fig. 9. Computer results for the reduction factor F' for the case $\Delta_1 = \Delta_2 = \Delta$

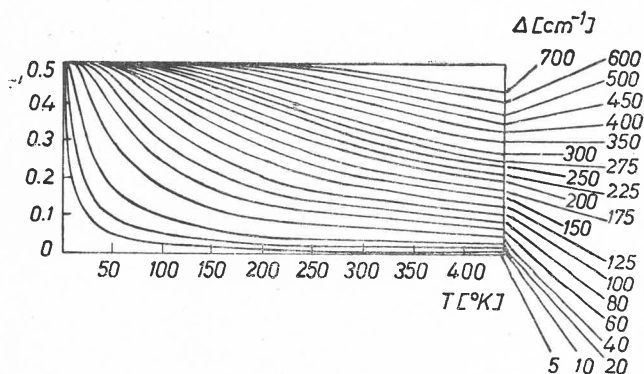


Fig. 10. Computer results for the reduction factor F' for the case $\Delta_1 = 0$, $\Delta_2 = \Delta$

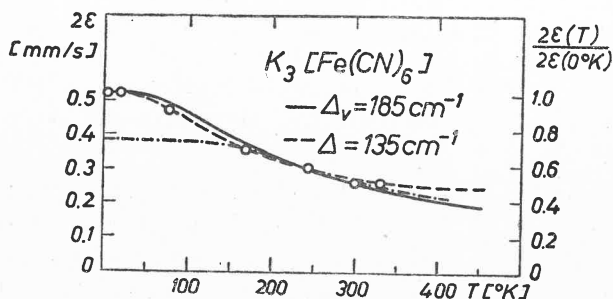


Fig. 11. Fitting of $K_3[\text{Fe}(\text{CN})_6]$ quadrupole splitting data

a [111] principal axis. The lattice contributions to quadrupole splitting are not larger than 0.35 mm/s. Summarizing the \hat{q}_v and \hat{q}_l tensors, one can calculate $F(\Delta, T)$ function which describes the temperature dependence of the quadrupole splitting, taking into account the lattice contribution. This function effects a change in comparison with $F'(\Delta, T)$ mainly when the valence electric field gradient is small, *viz.* at higher temperatures or for the case $F' \rightarrow 1/2$

when $T \rightarrow 0$. In such situations the lattice contribution markedly improves the fit (broken curves in Figs 2 to 7) and reduces Δ parameters.

Table I presents the parameters obtained in these investigations for cubic ferricyanides.

In Fig. 11 the fitting for $K_3[Fe(CN)_6]$ is presented. The dot-dash curve corresponds to Oosterhuis *et al.* [4]. The continuous curve corresponds to our estimates for the valence

TABLE I

$2\varepsilon(0^\circ K)$ is quadrupole splitting extrapolated to $0^\circ K$. Values of separation Δ_v between singlet and doublet orbital states are obtained from fitting experimental curves to valence gradient contribution, the values Δ — from fitting to resulting sum of valence and lattice gradients

$Me_3[Fe(CN)_6]_2$	$2\varepsilon(0^\circ K)$ [mm/s]	Δ_v [cm^{-1}]	Δ [cm^{-1}]
$Cu_3[Fe(CN)_6]_2$	0.80	280	250
$Ni_3[Fe(CN)_6]_2$	0.96	300	290
$Co_3[Fe(CN)_6]_2$	0.79	300	275
$Mn_3[Fe(CN)_6]_2$	0.92	215	200
$Cd_3[Fe(CN)_6]_2$	0.95	270	255
$Ca_3[Fe(CN)_6]_2$	0.49	260	180

gradient only. When the lattice contribution $2\varepsilon_l = 0.2$ mm/s is included in a similar way to cubic ferricyanides the fit is better and Δ reduces to ca. 135 cm^{-1} in good agreement with the results of other methods ($\Delta = 100$ cm^{-1} Ref. [6]). Analysis of the temperature dependence of the quadrupole splitting also confirms that in potassium ferricyanide the ground state is single and the higher state degenerate.

REFERENCES

- [1] B. Sawicka, J. Sawicki, A. Z. Hryniewicz, *Sol. Stat. Phys. (USSR)*, **9**, 1410 (1967).
- [2] A. K. van Bever, *Rec. Trav. Chim. Pays Bas*, **57**, 1259 (1938).
- [3] H. B. Weiser, W. O. Milligan, J. B. Bates, *J. Phys. Chem.*, **46**, 99 (1942).
- [4] W. T. Oosterhuis, G. Lang, S. DeBenedetti, *Phys. Letters*, **24A**, 346 (1967).
- [5] R. I. Ingalls, *Phys. Rev.*, **133A**, 787 (1964).
- [6] T. Ohtsuka, *J. Phys. Soc. Japan*, **16**, 1549 (1961).